Progress In Electromagnetics Research C, Vol. 131, 13–24, 2023

Compact 4-Port Vivaldi MIMO Antenna for 5G Wireless Devices

Golla Ramyasree* and Nelaturi Suman

Abstract—In this paper, a novel compact 4-port Vivaldi Multiple Input Multiple Output (MIMO) antenna is proposed for 5G wireless devices. The presented antenna has dimensions $40 \times 40 \times 1.6\,\text{mm}^3$. The suggested antenna is fabricated on RT/Duroid dielectric material with dielectric constant of 2.2. The orthogonal arrangement of antenna elements and embedding slits between them result in enhanced isolation. The gain observed for the proposed antenna is 2.405 dB. The diversity performance of the MIMO structure in terms of Envelop Correlation Coefficient (ECC < 0.02), Total Active Reflection Coefficient (TARC $< -10\,\text{dB}$), Diversity Gain (DG > 9.998), Channel capacity Loss (CCL < 0.4), and Mean Effective Gain (MEG $< 1\,\text{dB}$) is studied and analyzed. The simulated and measured results are in good agreement.

1. INTRODUCTION

Present 5G wireless communication systems require compact wide band MIMO antennas with enhanced isolation between the ports. MIMO antenna plays a crucial role to improve the transmission range without increasing the signal power with high efficiency, low latency, maximum throughput, and improved channel capacity [1]. By ITU-R norms 5G spectrum can be categorized as two frequency ranges, FR1 (Frequency Range1) and FR2 (Frequency Range 2). FR1 is below 6 GHz or sub-6 GHz offering 410 MHz–7125 MHz, and FR2 is above 6-GHz offering 24.25 GHz to 52.6 GHz. MIMO antennas are designed in these two frequency ranges, FR1 [8–18] and FR2 [19–25]. Utilizing conformal antenna arrays at the transmitter and receiver ends increases the MIMO system's capacity [2]. MIMO technology transfers more data more quickly by using many antennas at the transmitter and receiver [3]. To reduce the mutual coupling of two antennas resonating in adjacent frequency bands, an antenna interference cancellation chip with a high-pass response is proposed [4]. The mutual coupling between two densely packed dipole antennas is reduced, and cross-polarization suppression is ensured by the ceramic superstrate-based decoupling method [5]. The isolation of dual-polarized and wideband large-scale antenna arrays is enhanced using the non-resonant metasurface approach [6]. It is considered to utilize a 3-D metamaterial structure to minimize mutual coupling of a two-element patch antenna array [7]. In MIMO antenna , the isolation between elements and envelope correlation coefficient is important. A compact 4-port MIMO antenna is designed at 2.5 GHz applications, and for better isolation a square ring defected ground structure is inserted [11]. A unitcell metamaterial is introduced [13], and the four elements of a slotted ground plane antenna are arranged orthogonally for better correlation [12]. Orthogonal polarization technique is used for better mutual coupling effect, but for 2 elements, the proposed antenna occupies a large area [14].

Gibson introduced Vivaldi antennas or tapered slot antennas in 1979 [26]. These Vivaldi antennas are also called broadband antennas because they provide wide bandwidth. Vivaldi antennas are mostly available in 3D models [27]. By using 3D models the size is a complex factor, so here reducing the size complexity of Vivaldi antennas, printed Vivaldi antennas [28–30] have been used.

Received 28 January 2023, Accepted 23 February 2023, Scheduled 11 March 2023

* Corresponding author: Golla Ramyasree (ramyasree.golla@gmail.com).

The authors are with the Department of Electronics and Communication Engineering, VFSTR (Deemed to be University), Vadlamudi, Andhra Pradesh, India.

Vivaldi antennas were also used for 5G applications [31–35], and mostly printed Vivaldi antenna arrays have been used for these applications [36–39]. A Vivaldi antenna is designed for 4G/5G wireless devices [38]. In this paper, firstly, a single element Vivaldi antenna is designed at resonant frequency 3.5 GHz and compact in size compared with a monopole antenna [40]. Then, a novel 4-port MIMO Vivaldi antenna is designed at resonant frequency 3.5 GHz, and it has better MIMO performance characteristics than the 4-port monopole antenna which contains electromagnetic band gap (EBG) structures [41]. Here a 4-port Vivaldi antenna is presented with compactness in size and executed with better MIMO characteristics. Simulations are carried out in HFSS Software.

2. ANTENNA PARAMETRIC STUDY

MIMO communication uses numerous antennas to transfer the same data as multiple signals using only one radio channel. RF link's signal quality and strength are increased using numerous antennas in this instance of antenna diversity. At the transmission point, the data are divided into several data streams that are then recombined on the receiving side by another MIMO radio setup with the same number of antennas. Different methods for improving the isolation in MIMO antennas have been described [3–6, 11]. The proposed method achieves improved isolation by arranging the antenna elements orthogonally. The proposed 4-port Vivaldi antenna with size 40×40 mm is designed on Rogers RT/Duroid 5880(tm) material with thickness 1.6 mm which is shown in Fig. 2, and the single element antenna is shown in Fig. 1(a). The Vivaldi structure acts as a defected ground structure (DGS), and elements are arranged orthogonally in ground plane to get better isolation which is one of the main techniques used in recent times. General microstrip feed line structure is changed to get exact resonant frequency. By adopting this Vivaldi structure, the antenna is compact compared with existing systems. A basic Vivaldi antenna is designed with the help of exponential curve. The exponential tapered slot is defined by using opening rate 'r', and two points $P_1\,(x_1, y_1)$ and $P_2\,(x_2, y_2)$ [28] can be expressed as

$$y = c_1 e^{rx} + c_2 \tag{1}$$

$$C_1 = \frac{(y_2 - y_1)}{e^{rx_2} - e^{rx_1}} \tag{2}$$

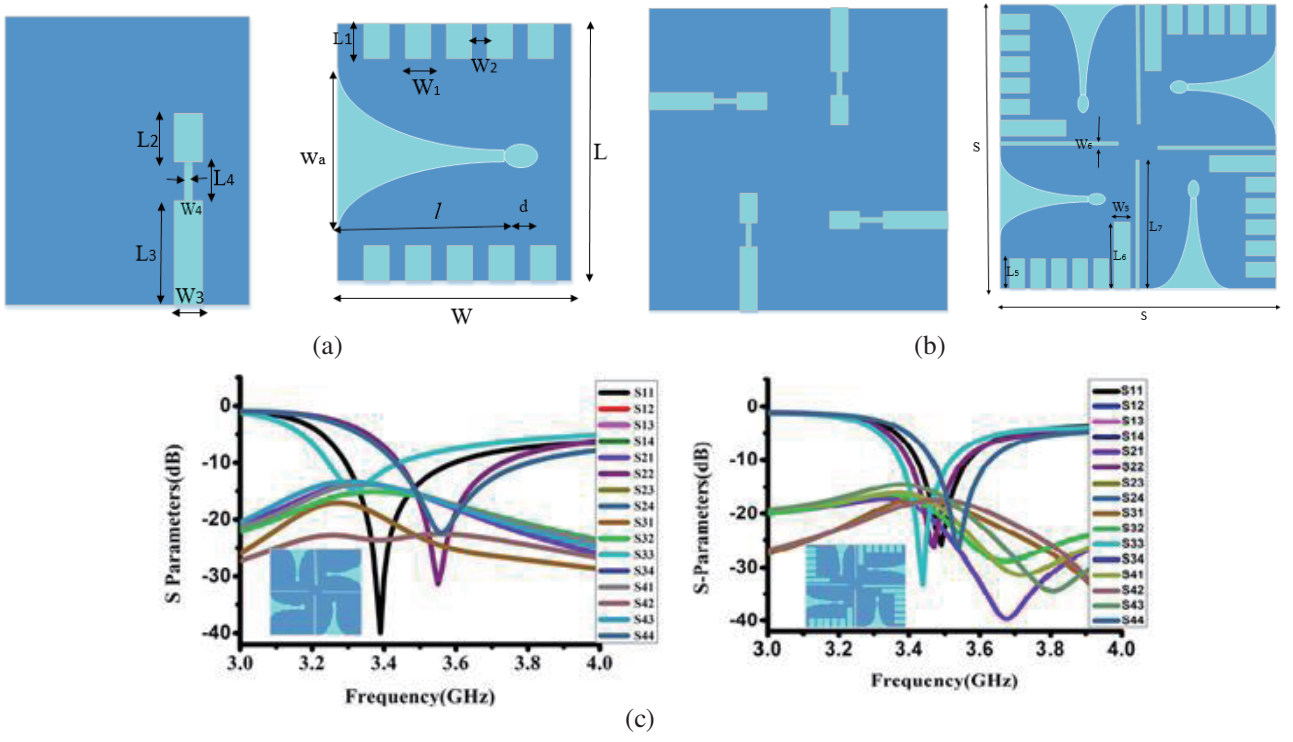

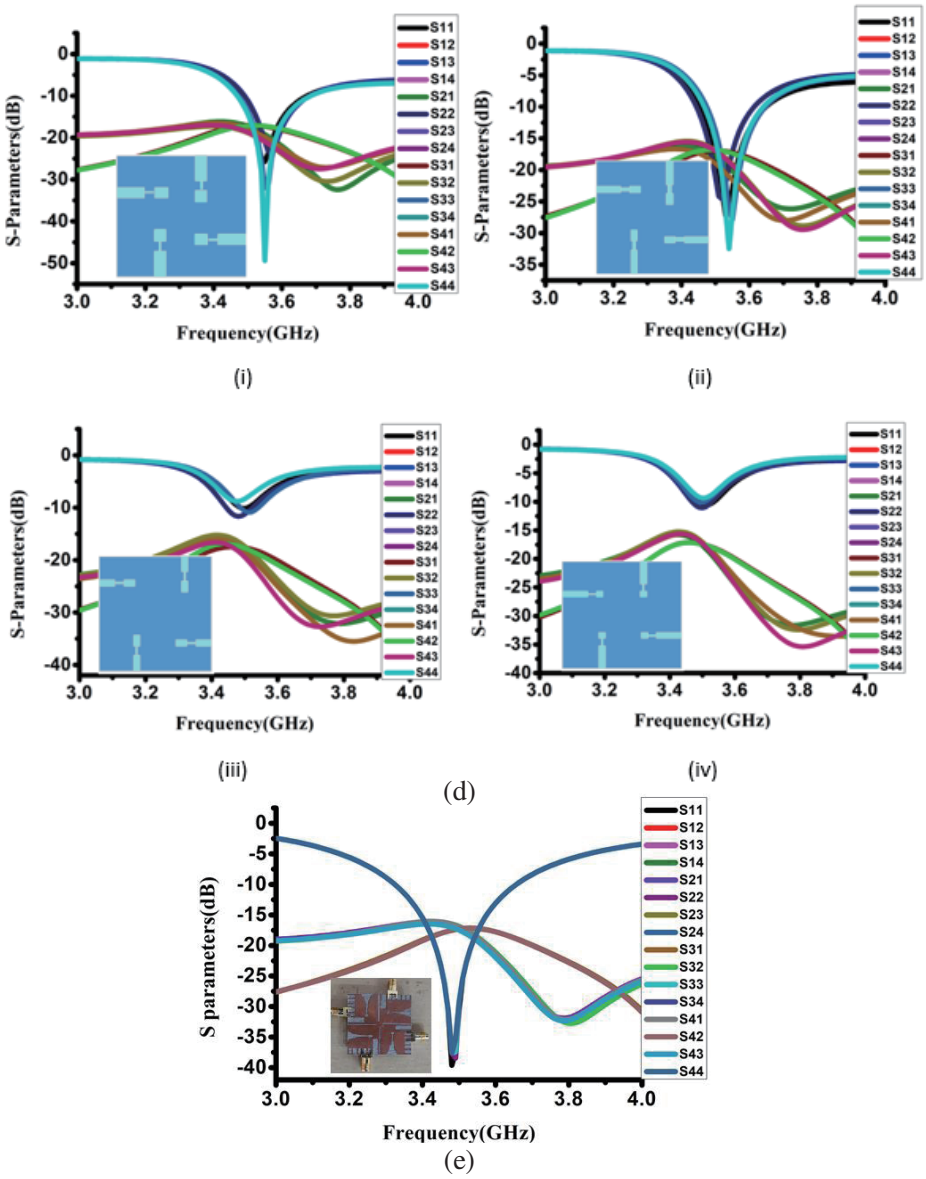

Figure 1. Proposed 4-port Vivaldi MIMO antenna and their corresponding results (a) Single element front view and back view (b) 4-element front view and back view (c) S-parameter results of 4-port Vivaldi antenna without slits and Aperture width variation ($W_a = 5.262\,\text{mm}$) (d) S-parameters w.r.t changes in feedline structure (i) $W_3 = 2.4\,\text{mm}$ (ii) $W_4 = 0.7\,\text{mm}$ (iii) $L_3 = 6\,\text{mm}$ (iv) $L_2 = 2\,\text{mm}$ (e) S-parameter results with slits ($Wa = 6.875\,\text{mm}$, $W_3 = 1.8\,\text{mm}$, $W_4 = 0.35\,\text{mm}$, $L_3 = 6\,\text{mm}$, $L_2 = 2\,\text{mm}$).

$$C_2 = \frac{(y_1 e^{rx_2} - y_2 e^{rx_1})}{e^{rx_2} - e^{rx_1}} \tag{3}$$

Here C_1 and C_2 are defined using points $P_1\,(x_1, y_1)$ and $P_2\,(x_2, y_2)$. Aperture width (W_a) is calculated by using the given formula

$$W_a = \frac{c}{f_{\min}\sqrt{\varepsilon_r}} \tag{4}$$

c — Speed of light and ε_r — Dielectric material constant.

As W_a changes, the resonant frequency of the S-parameter changes, making it challenging to achieve perfect matching, as seen in Fig. 1(c). Therefore, we opted at $W_a = 6.875\,\text{mm}$ to achieve perfect matching. The microstrip feedline structure of the suggested antenna's front view is studied to

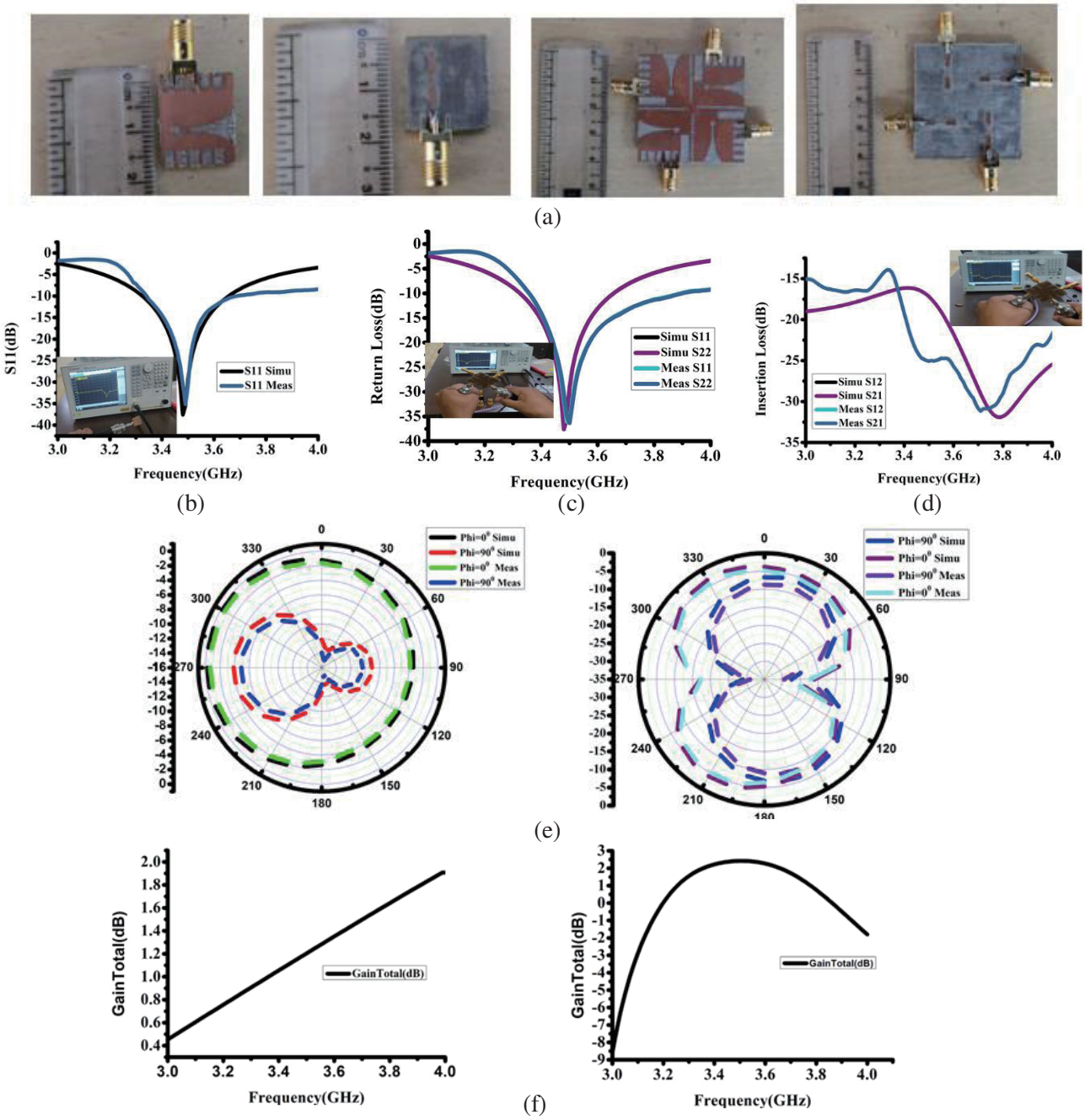

Figure 2. Fabricated Model and Measurement Results. (a) Fabricated model of single element and 4-port Vivaldi MIMO antenna. (b) Measured single element S_{11}. (c) Measured S_{11}& S_{22} of 4-port Vivaldi MIMO antenna. (d) Measured S_{12} & S_{21} of 4-port Vivaldi MIMO antenna. (e) Co and cross polarizations of H and E planes. (f) Gain (vs) Frequency plots of single element and MIMO antenna.

obtain the optimal bandwidth, as shown in Fig. 1(b). Various parametric changes are made with feedline structure shown in Fig. 1(d). Correlation was increased whether antenna elements were positioned in the same direction or the opposite direction. Here, antenna elements are positioned orthogonally to get better correlation and to minimise the size of the antenna seen in Fig. 1(b). Slits are added at the sides of the antenna, different numerous parametric analyses are done to obtain perfect matching and greater isolation, as illustrated in Fig. 1(e).

2.1. Decoupling Mechanism of Antenna

Expelling the flowing currents between the antenna elements is the foundation of the suggested decoupling concept. To do this, the device has a tapered groove etched into the ground plane, seen in Fig. 2(b). Based on the travelling wave operating theory, the antenna permits extracting currents and expels them outside [42]. As a result, ground currents can only flow longitudinally through the tapered slot and cannot travel transversely from one antenna to another antenna. The proposed antenna parameters dimensions are shown in Table 1.

Table 1.

Parameter	Value (mm)	Parameter	Value (mm)	Parameter	Value (mm)	Parameter	Value (mm)
L	18	L_5	4	W_1	2	W_6	0.8
L_1	3	L_6	10	W_2	1	W_a	6.845
L_2	4	L_7	18	W_3	1.8	l	13.5
L_3	8	L_8	22	W_4	0.35	d	2
L_4	3.8	W	18	W_5	3	S	40

3. RESULTS AND DISCUSSIONS

The proposed antenna is made of Rogers RT/Duroid material. Fabricated model of the proposed single element and 4-port Vivaldi MIMO antenna is shown in Fig. 2(a). The 4-port MIMO antenna's simulated scattering parameters are taken, and they are compared to the measured scattering parameters. The network analyzer used to measure all of the S-parameters can measure up to 14 GHz. An anechoic chamber with the dimensions of $22.5 \times 12.5 \times 11.5\,\text{mm}^3$ and operating at a frequency range of 400 MHz to 18 GHz is used for the measurements.

Figure 1(e) shows all of the 2×2 MIMO antenna's simulated scattering parameters, and S_{11} here indicates the reflection coefficient when port 1 is excited. Similarly, S_{22}, S_{33}, and S_{44} represent reflection coefficients when ports 2, 3, and 4 are excited. It is possible to see the return loss for all four scattering parameters at -10 dB below from 3.33 to 3.66 GHz. Fig. 2(b) shows the comparison plot of the single element Vivaldi antenna's simulated and measured S_{11} parameter. One can see the high reflection coefficient, or -35.44 dB, at 3.5 GHz, and it is operated in 3.36–3.389 GHz band with respect to measurements. When two ports are excited, these simulated results are then compared to the measured scattering parameters. At the resonant frequency of 3.5 GHz, the measured S_{11} & S_{22} are -35.93 dB and -36.34 dB, respectively, while the simulated S_{11} & S_{22} are -29.22 dB and observed measured return loss below -10 dB from 3.36 GHz to 3.81 GHz as shown in Fig. 2(c).

At the resonant frequency of 3.5 GHz, the measured S_{12} & S_{21} are -25.06 dB and -25.07 dB, respectively, and they are better than [11, 13], while the simulated S_{12} & S_{21} are -17.19 dB and observed measured insertion loss below -15 dB from 3.36 GHz to 4 GHz as shown in Fig. 2(d). According to the measured results in Fig. 2(d), the high isolation of -25.06 dB is attained due to antenna ground plane structure. Fig. 2(e) shows the radiation patterns of both the H- and E-planes, as they were simulated and measured. Phi(ϕ) = 0° & 90° in the H-plane represent co- and cross-polarizations. Co- and cross-polarizations are represented in the E-plane by Phi(ϕ) = 90° & 0°. From Fig. 2(f) it can be observed that the gain for single element is 1.203 dB at 3.5 GHz, and the gain for 4-port MIMO Vivaldi antenna is 2.405 dB.

The surface current distribution of a 4-port Vivaldi MIMO antenna is shown in Fig. 3. When ports 1, 2, 3, and 4 are excited from Fig. 3(a) to Fig. 3(d), it is possible to view the current distribution of the antenna's front view at the resonant frequency of 3.5 GHz. Look at the etched Vivaldi structure's ground plane current distribution in Fig. 3(e), which is presented when all ports are excited at the resonant frequency of 3.5 GHz.

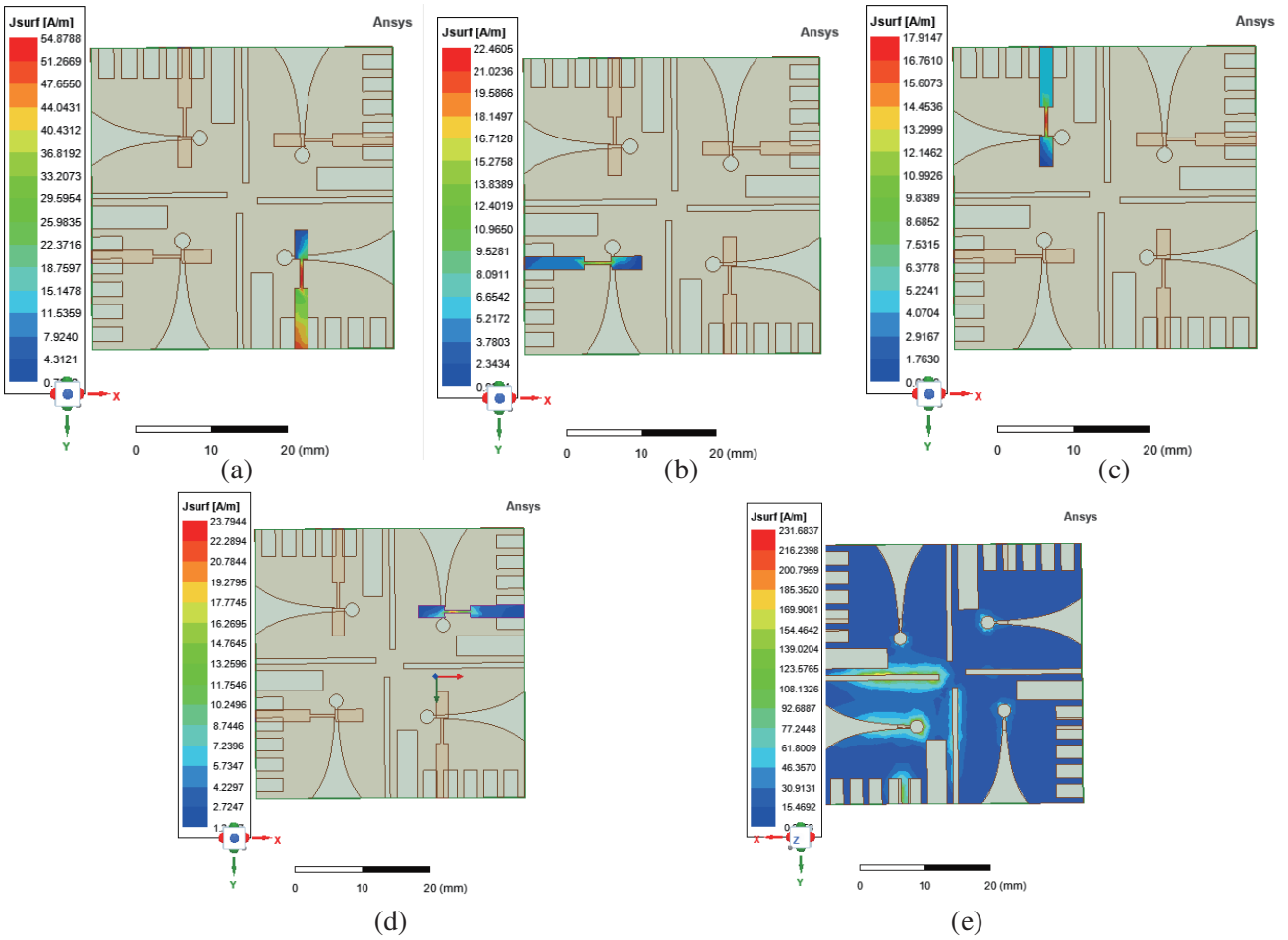

Figure 3. Surface current distribution of 4-port Vivaldi MIMO antenna. (a) Port-1. (b) Port-2. (c) Port-3. (d) Port-4 are excited shown in back view. (e) Port-1 is excited shown in front view.

3.1. MIMO Performance Parameters

The most crucial factors to consider while evaluating the MIMO antenna performance are:

i ECC (Envelope correlation coefficient)
ii DG (Diversity gain)
iii TARC (Total active reflection coefficient)
iv CCL (Channel Capacity Loss)
v MEG (Mean effective gain)

3.1.1. Envelope Correlation Coefficient

One important parameter in MIMO antennas is ECC. ECC can be estimated using S-parameters or by deriving radiation patterns using the provided formulas, which are stated as

$$\text{ECC or } \rho_{ij} = \frac{\left|S_{ii}^{*}S_{ij} + S_{ji}^{*}S_{jj}\right|^{2}}{\left(1 - |S_{ii}|^{2} - |S_{ji}|^{2}\right)\left(1 - |S_{jj}|^{2} - |S_{ij}|^{2}\right)} \tag{5}$$

$$\mathrm{ECC} = \frac{\left|\iint \vec{E_1}(\theta,\varphi)\cdot\vec{E_2^*}(\theta,\varphi)\,d\Omega\right|^2}{\iint\left|\vec{E_1^*}(\theta,\varphi)\right|^2 d\Omega \iint\left|\vec{E_2^*}(\theta,\varphi)\right|^2 d\Omega} \tag{6}$$

Typically, the ECC is calculated between two antenna elements. The correlation standard value is essentially less than 0.5. Here, ECC is estimated between antenna elements (1, 2), (1, 3), (1, 4), (2, 3), (2, 4), and (3, 4). ECC 0.01 can be seen in the simulated results shown in Fig. 4(a) for all of these antenna elements.

3.1.2. Diversity Gain

Diversity gain describes how much transmitted power is lowered whenever the diversity concept is used. DG is determined using the equation below.

$$\mathrm{DG} = 10\sqrt{1-|\rho_{ij}|^2} \tag{7}$$

When the DG value of a MIMO antenna is 10, the diversity performance of the antenna is good. One can see in Fig. 4(b) that the DG value is greater than 9.99 for the specified frequency range and calculated between the (1, 2), (1, 3), (1, 4), (2, 3), (2, 4), and (3, 4) antenna elements.

3.1.3. Total Active Reflection Coefficient

TARC is defined as ratio of square root of total reflected power to the total incident power. TARC at N-port [31] can be expressed as

$$\Gamma_a^t \frac{\sqrt{\sum_{i=1}^{N}|b_i|^2}}{\sqrt{\sum_{i=1}^{N}|a_i|^2}} \tag{8}$$

Here a_i is the incident signal and b_i the reflected signal. For 1×2 MIMO antenna scattering matrix can be expressed as

$$\begin{bmatrix} b_1 \\ b_2 \end{bmatrix} = \begin{bmatrix} S_{11} & S_{12} \\ S_{21} & S_{22} \end{bmatrix}\begin{bmatrix} a_1 \\ a_2 \end{bmatrix} \tag{9}$$

Reflected signals are characterized by Gaussian random variables as

$$b_1 = s_{11}a_1 + s_{12}a_2 = s_{11}a_0e^{j\theta_1} + s_{12}a_0e^{j\theta_2} = a_1\left(s_{11}+s_{12}e^{j\theta}\right) \tag{10}$$

$$b_2 = s_{21}a_1 + s_{22}a_2 = s_{21}a_0e^{j\theta_1} + s_{22}a_0e^{j\theta_2} = a_1\left(s_{21}+s_{22}e^{j\theta}\right) \tag{11}$$

Mainly TARC is used to observe the effective reflection coefficient of MIMO systems. For 1×2 MIMO antenna TARC can be expressed as

$$\Gamma_a^t = \sqrt{\frac{\left|a_1\left(s_{11}+s_{12}e^{j\theta}\right)\right|^2 + \left|a_1\left(s_{21}+s_{22}e^{j\theta}\right)\right|^2}{2\left|a_1\right|^2}} \tag{12}$$

$$\Gamma_a^t = \sqrt{\frac{\left|\left(s_{11}+s_{12}e^{j\theta}\right)\right|^2 + \left|\left(s_{21}+s_{22}e^{j\theta}\right)\right|^2}{2}} \tag{13}$$

$$\Gamma_a^t = \sqrt{\frac{\left|\left(s_{11}+s_{12}\right)\right|^2 + \left|\left(s_{21}+s_{22}\right)\right|^2}{2}} \tag{14}$$

TARC is calculated between (1, 2), (1, 3), (1, 4), (2, 3), (2, 4) and (3, 4) antenna elements and is shown in Fig. 4(c).

3.1.4. Channel Capacity Loss

During correlation effect, MIMO system provides the information about channel capacity losses. CCL standard practical value is 0.4 bits/s/Hz. From Fig. 4(d) the value below 0.4 can be observed for specified frequency range. CCL is calculated between (1, 2), (1, 3), (1, 4), (2, 3), (2, 4), and (3, 4) antenna elements. CCL can be mathematically calculated as

$$C_{loss} = -\log_2 \det\left(\varphi^R\right) \tag{15}$$

$$\varphi^R = \begin{bmatrix} \rho_{11} & \rho_{12} \\ \rho_{21} & \rho_{22} \end{bmatrix} \tag{16}$$

$$\rho_{ii} = 1 - \left(|s_{ii}|^2 + |s_{ij}|^2\right) \tag{17}$$

$$\rho_{ij} = -\left(s_{ii}^* s_{ij} + s_{ji}^* s_{jj}\right) \tag{18}$$

where φ^R is the correlation matrix.

3.1.5. Mean Effective Gain

Mean effective gain is one of the important parameters in a MIMO system. MEG calculates mean received power in fading environment. It is mathematically calculated as [21]

$$\mathrm{MEG}_i = 0.5\mu_{irad} = 0.5\left(1 - \sum_{j=1}^{K} |s_{ij}|^2\right) \tag{19}$$

where K is the number of antennas, and the MEG value should be $-3\,\mathrm{dB} \leq \mathrm{MEG} < -12\,\mathrm{dB}$. For four antenna elements, the MEG value is shown in Fig. 4(e), and MEG value is in between $-3\,\mathrm{dB}$ & $-12\,\mathrm{dB}$ for specified frequency range. For any two antenna elements if we take MEG ratio $\left(\frac{\mathrm{MEG}_i}{\mathrm{MEG}_j}\right)$, the value

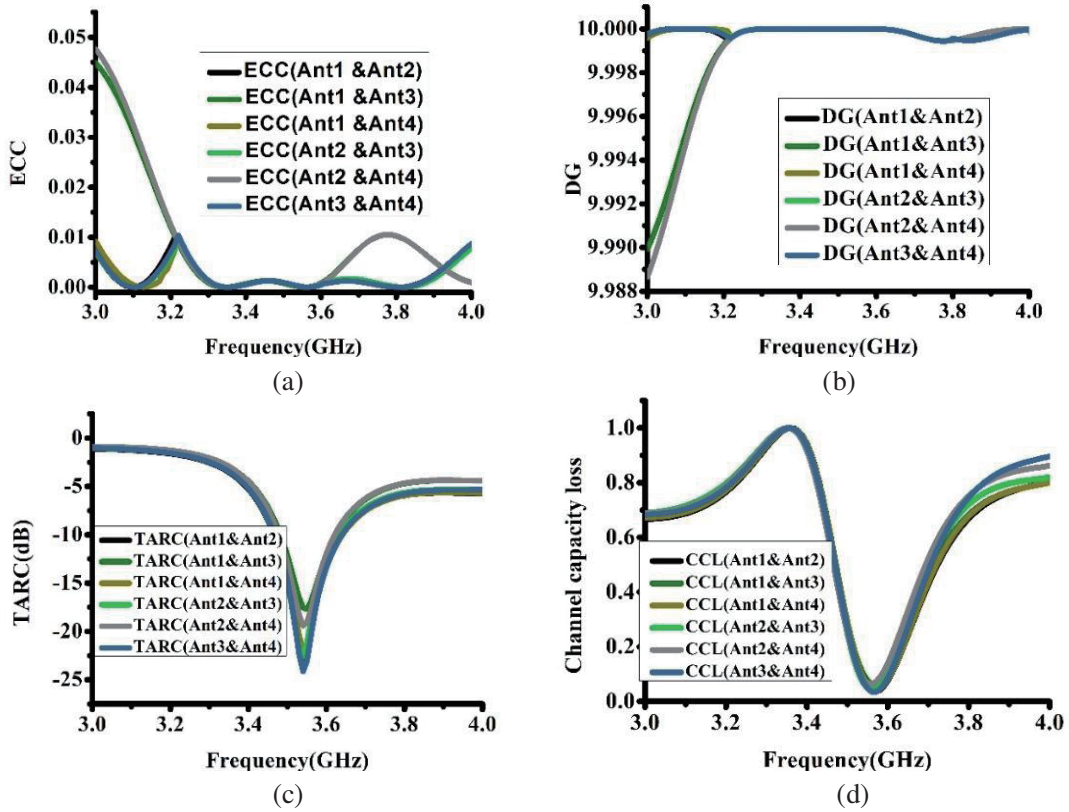

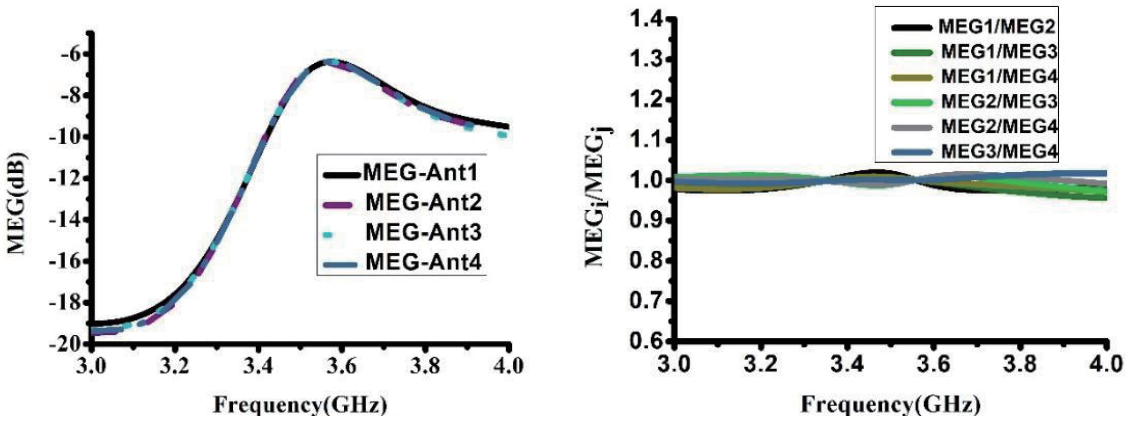

Figure 4. 4-port MIMO Vivaldi antenna performance characteristics. (a) ECC. (b) DG. (c) TARC. (d) CCL. (e) MEG of Individual Elements. (f) Ratio of MEG.

should be $\leq \pm 3$ dB and is observed in Fig. 4(f). It is noticed that MEG ratio is calculated for the (1, 2), (1, 3), (1, 4), (2, 3), (2, 4), and (3, 4) antenna elements.

Table 2 represents the comparison table with existing systems.

Table 2.

Ref	Operating Band	No of antenna elements	Size	Isolation (dB)	ECC
[11]	2.44–2.48	4	$60 \times 60\,\text{mm}^2$	Below -24	< 0.1
[12]	2.2–6.28	4	$45 \times 45\,\text{mm}^2$	Below -14	< 0.1
[13]	5.7–5.85	2	$44 \times 37\,\text{mm}^2$	Below -24.5	< 0.1
[14]	3.0-6.3	2	$38 \times 25\,\text{mm}^2$	Below -35	< 0.02
[17]	4.65–4.97	2	$50 \times 35\,\text{mm}^2$	Below -17	< 0.03
[39]	3.31–3.68	10-array	$450 \times 140\,\text{mm}^2$	N/A	N/A
[41]	3.37–3.67	4	$60 \times 60\,\text{mm}^2$	Below -17	< 0.1
Proposed	3.33–3.66	4	$40 \times 40\,\text{mm}^2$	Below -17.5	< 0.01

4. CONCLUSION

A brand-new, compact Vivaldi MIMO antenna is suggested for 5G wireless devices. Simulated and measured results are compared for a compact Vivaldi MIMO antenna, and a fabricated 4-port Vivaldi MIMO antenna below -10 dB return loss is obtained from 3.36 to 3.90 GHz. Next, a small 2×2 MIMO Vivaldi antenna is created, and according to measurements, it operates between 3.36 and 3.89 GHz. The antenna exhibits -25.06 dB isolation at the resonant frequency. As per calculations of the MIMO antenna performance parameters, the proposed antenna produces the best results with ECC 0.01, DG > 9.99, CCL 0.4, TARC -10 dB, and MEG is between -3 dB & -12 dB for the specified frequency range.

REFERENCES

1. Kumar, S., A. S. Dixit, R. R. Malekar, H. D. Raut, and L. K. Shevada, "Fifth generation antennas: A comprehensive review of design and performance enhancement techniques," *IEEE Access*, Vol. 8, 163568–163593, 2020, doi: 10.1109/ACCESS.2020.3020952.
2. Recioui, A., "Capacity optimization of MIMO systems involving conformal antenna arrays using a search group algorithm," *Algerian Journal of Signals and Systems*, Vol. 5, No. 4, 209–214, 2020.
3. Recioui, A. and Y. Grainat, "Application and optimization of MIMO communication in wide area monitoring systems," *International Journal of Data Science*, Vol. 1, No. 2, 82–98, 2020.
4. Zhao, L., F. Liu, X, Shen, et al., "A high-pass antenna interference cancellation chip for mutual coupling reduction of antennas in contiguous frequency bands," *IEEE Access*, Vol. 6, 38097–38105, 2018.
5. Liu, F., J. Guo, L. Zhao, et al., "Ceramic superstrate-based decoupling method for two closely packed antennas with cross-polarization suppression," *IEEE Transactions on Antennas and Propagation*, Vol. 69, No. 3, 1751–1756, 2020.
6. Luo, S., P. Mei, Y. Zhang, G. F. Pedersen, and S. Zhang, "Decoupling of dual-polarized antenna arrays using non-resonant metasurface," *Sensors*, Vol. 23, No. 1, 152, Dec. 2022, doi: 10.3390/s23010152.
7. Kai, Y., Y. Li, and X. Liu, "Mutual coupling reduction of a MIMO antenna array using 3-D novel meta-material structures," *The Applied Computational Electromagnetics Society Journal (ACES)*, 758–763, 2018.
8. Guo, J., F. Liu, L. Zhao, et al., "Meta-surface antenna array decoupling designs for two linear polarized antennas coupled in H-plane and E-plane," *IEEE Access*, Vol. 7, 100442–100452, 2019.
9. Chae, S. H., S. Oh, and S. Park, "Analysis of mutual coupling, correlations, and TARC in WiBro MIMO array antenna," *IEEE Antennas and Wireless Propagation Letters*, Vol. 6, 122–125, 2007, doi: 10.1109/LAWP.2007.893109.
10. Yang, L., T. Li, and S. Yan, "Highly compact MIMO antenna system for LTE/ISM applications," *International Journal of Antennas and Propagation*, 2015, https://doi.org/10.1155/2015/714817.
11. Anitha, R., S. Mathew, P. V. Vinesh, P. Mohanan, and K. Vasudevan, "Compact 4 port MIMO antenna using polarization and pattern diversity," *2015 IEEE 16th Annual Wireless and Microwave Technology Conference (WAMICON)*, 1–4, 2015, doi: 10.1109/WAMICON.2015.7120360.
12. Anitha, R., P. V. Vinesh, K. C. Prakash, P. Mohanan, and K. Vasudevan, "A compact quad element slotted ground wideband antenna for MIMO applications," *IEEE Transactions on Antennas and Propagation*, Vol. 64, No. 10, 4550–4553, Oct. 2016, doi: 10.1109/TAP.2016.2593932.
13. Iqbal, A., O. A Saraereh, A. Bouazizi, and A. Basir, "Metamaterial-based highly isolated MIMO antenna for portable wireless applications," *Electronics*, Vol. 7, No. 10, 267, Oct. 2018, doi: 10.3390/electronics7100267.
14. Sree, G. N. J. and S. Nelaturi, "Opportunistic control of crescent shape MIMO design for lower sub 6 GHz 5G applications," *Microw Opt Technol Lett.*, Vol. 64, 896–904, 2022, doi:10.1002/mop.33211.
15. Gomase, R. and S. Nandi, "A circular patch dual-band MIMO antenna for sub-6 GHz applications," *2019 IEEE Indian Conference on Antennas and Propogation (InCAP)*, 1–4, 2019, doi: 10.1109/InCAP47789.2019.9134499.
16. Krishnamoorthy, R., A. Desai, R. Patel, et al., "4 element compact triple band MIMO antenna for sub-6 GHz 5G wireless applications," *Wireless Netw*, Vol. 27, 3747–3759, 2021, https://doi.org/10.1007/s11276-021-02734-8.
17. Desai, A., et al., "Transparent 2-element 5G MIMO antenna for sub-6 GHz applications," *Electronics*, Vol. 11, No. 2, 251, Jan. 2022, doi: 10.3390/electronics11020251.
18. Sree, G. N. J. and S. Nelaturi, "Design and experimental verification of fractal based MIMO antenna for lower sub 6-GHz 5G applications," *AEU-International Journal of Electronics and Communications*, Vol. 137, 153797, 2021.

19. Wang, F., Z. Duan, X. Wang, et al., "High isolation millimeter-wave wideband MIMO antenna for 5G communication," *International Journal of Antennas and Propagation*, 2019, https://doi.org/10.1155/2019/4283010.
20. Khandelwal, M. and K. Binod, "Implementation of four-port MIMO diversity microstrip antenna with suppressed mutual coupling and cross-polarized radiations," *Microsystem Technologies*, 993–1000, doi: 10.1007/s00542-019-04574-1.
21. Khalid, M., S. I. Naqvi, N. Hussain, et al., "4-port MIMO antenna with defected ground structure for 5G millimeter wave applications," *Electronics*, Vol. 9, No. 1, 71, Jan. 2020, doi: 10.3390/electronics9010071.
22. Sehrai, D. A., M. Abdullah, A. Altaf, et al., "A novel high gain wideband MIMO antenna for 5G millimeter wave applications," *Electronics*, Vol. 9, No. 6, 1031, Jun. 2020, doi: 10.3390/electronics9061031.
23. Amrutha, P., K. L. V. Prasad, and S. Kumar, "Highly isolated fork-shaped MIMO antenna for 5G application," *2021 Asian Conference on Innovation in Technology (ASIANCON)*, 1–4, 2021, doi: 10.1109/ASIANCON51346.2021.9545004.
24. Hussain, N., W. A. Awan, W. Ali, S. I. Naqvi, A. Zaidi, and T. T. Le, "Compact wideband patch antenna and its MIMO configuration for 28 GHz applications," *AEU — International Journal of Electronics and Communications*, Vol. 132, 2021, https://doi.org/10.1016/j.aeue.2021.153612.
25. Fan, C., B. Wu, Y. Hu, Y. Zhao, and T. Su, "Millimeter-wave pattern reconfigurable Vivaldi antenna using tunable resistor based on graphene," *IEEE Transactions on Antennas and Propagation*, Vol. 68, No. 6, 4939–4943, Jun. 2020, doi: 10.1109/TAP.2019.2952639.
26. Gibson, P. J., "The Vivaldi aerial," *1979 9th European Microwave Conference*, 101–105, 1979, doi: 10.1109/EUMA.1979.332681.
27. Gjokaj, V., J. Papapolymerou, J. D. Albrecht, B. Wright, and P. Chahal, "A compact receive module in 3-D printed Vivaldi antenna," *IEEE Transactions on Components, Packaging and Manufacturing Technology*, Vol. 10, No. 2, 343–346, Feb. 2020, doi: 10.1109/TCPMT.2019.2961345.
28. Shan, J., A. Xu, and J. Lin, "A parametric study of microstrip-fed Vivaldi antenna," *2017 3rd IEEE International Conference on Computer and Communications (ICCC)*, 1099–1103, 2017, doi: 10.1109/CompComm.2017.8322713.
29. Li, Z., C. Yin, and X. Zhu, "Compact UWB MIMO Vivaldi antenna with dual band-notched characteristics," *IEEE Access*, Vol. 7, 38696–38701, 2019, doi: 10.1109/ACCESS.2019.2906338.
30. Li, Q. and Y. Sun, "A high isolation UWB MIMO antenna based on angle diversity," *2020 IEEE MTT-S International Wireless Symposium (IWS)*, 1–3, 2020, doi: 10.1109/IWS49314.2020.9360073.
31. Fritz-Andrade, E., H. Jardon-Aguilar, and J. A. Tirado-Mendez, " The correct application of total active reflection coefficient to evaluate MIMO antenna systems and its generalization to N ports," *Int. J. RF Microw. Comput. Aided Eng.*, 30:e22113, 2020, https://doi.org/10.1002/mmce.22113.
32. Elsheakh, D. M. and E. A. Abdallah, "Ultrawideband Vivaldi antenna for DVB-T, WLAN and WiMAX applications," *Research Article in International Journal of Antennas and Propagation*, 2014, http://dx.doi.org/10.1155/2014/761634.
33. Zhu, Y., D. Su, W. Xie, Z. Liu, and K. Zuo, "Design of a novel miniaturized Vivaldi antenna with loading resistance for ultra wideband (UWB) applications," *ACES Journal*, Vol. 32, No. 10, 895–900, Jul. 2021.
34. Paul, L. C. and M. M. Islam, " A super wideband directional compact Vivaldi antenna for lower 5G satellite applications," *Research Article in International Journal of Antennas and Propagation*, 2021, https://doi.org/10.1155/2021/8933103
35. Ren, J., H. Fan, Q. Tang, Z. Yu, Y. Xiao, and X. Zhou, "An ultra-wideband Vivaldi antenna system for long-distance electromagnetic detection," *Applied Sciences*, Vol. 12, No. 1, 528, Jan. 2022, doi: 10.3390/app12010528.
36. Ojaroudiparchin, N., M. Shen, and G. F. Pedersen, "Design of Vivaldi antenna array with end-fire beam steering function for 5G mobile terminals," *2015 23rd Telecommunications Forum Telfor (TELFOR)*, 587–590, 2015, doi: 10.1109/TELFOR.2015.7377536.

37. Zhu, S., H. Liu, Z. Chen, and P. Wen, "A compact gain-enhanced Vivaldi antenna array with suppressed mutual coupling for 5G mmWave application," *IEEE Antennas and Wireless Propagation Letters*, Vol. 17, No. 5, 776–779, May 2018, doi: 10.1109/LAWP.2018.2816038.
38. Ikram, M., N. Nguyen-Trong, and A. M. Abbosh, "Realization of a tapered slot array as both decoupling and radiating structure for 4G/5G wireless devices," *IEEE Access*, Vol. 7, 159112–159118, 2019, doi: 10.1109/ACCESS.2019.2950660.
39. Truong, L., G. Truong, and T. Tran, "A new linear printed Vivaldi antenna array with low side lobe level and high gain for the band 3.5 GHz," *REV Journal on Electronics and Communications*, 2020, doi: 10.10.21553/rev-jec.247.
40. Aathmanesan, T., "Novel slotted hexagonal patch antenna for sub-6 GHz 5G wireless applications," *ICTACT Journal on Microelectronics*, 1010–1013, 2021, doi: 10.21917/ijme.2021.0176.
41. Mishra, M., S. Chaudhuri, and R. S. Kshetrimayum, "Low mutual coupling four-port MIMO antenna array for 3.5 GHz WiMAX application," *2020 IEEE Region 10 Symposium (TENSYMP)*, 791–794, 2020, doi:10.1109/TENSYMP50017.2020.923104.
42. Tebache, S., A. Belouchrani, F. Ghanem, and A. Mansoul, "Novel reliable and practical decoupling mechanism for strongly coupled antenna arrays," *IEEE Transactions on Antennas and Propagation*, Vol. 67, No. 9, 5892–5899, Sept. 2019, doi: 10.1109/TAP.2018.2885.